Jupiter's Red Spot

Luke McGuire
Program in Applied Mathematics
University of Arizona

May 21, 2009

Abstract

The Great Red Spot, the largest of Jupiter's long lived, approximately two dimensional, coherent vortices, measures approximately $26,000 \times 13,000$ km in the horizontal direction and is assumed to be roughly 20-40 km deep. Previous studies, including laboratory experiments and numerical simulations, suggest that many of the important characteristics of Jovian vortices can be explained through quasi-geostrophic theory. Based on work by Phillip Marucs, a simple two layer model of the Jovian atmosphere is developed in which vortices lie in a thin layer of the atmosphere above a much deeper, time independent flow. The lower layer only influences the upper layer by changing its vertical depth. The fluid in the upper layer is assumed to be homogeneous and incompressible. Starting with the full momentum equation, standard scaling arguments are used to motivate the quasi-geostrophic and hydrostatic equations. From the approximate horizontal momentum equations, the conservation of potential vorticity is derived and used in a model for Jovian vortices. The resulting system is solved numerically using a combination of Galerkin and finite difference methods. Data from several simulations is presented and compared with previous results.

1 Introduction

In a reference frame rotating with the planetary angular velocity, Ω, the momentum equation can be written as

$$\frac{D\mathbf{u}}{Dt} + 2\mathbf{\Omega} \times \mathbf{u} = \frac{-\nabla p}{\rho} + \nabla\Phi + \frac{\mathbf{F}}{\rho} \tag{1}$$

where ρ is the density, p the pressure, the term $2\mathbf{\Omega} \times \mathbf{u}$ is referred to as the Coriolis force, and $\mathbf{u} = (u, v, w)$ is the fluid velocity with components u,v, and w in the east, north, and vertical directions respectively. The operator $\frac{D}{Dt}$ denotes the material derivative, $\frac{D}{Dt} = \frac{\partial}{\partial t} + \mathbf{u} \cdot \nabla$, and gravity and centripetal acceleration are represented through the gradient of the potential function, Φ. The frictional force is

$$\mathbf{F} = \mu\nabla^2\mathbf{u} + \frac{\mu}{3}\nabla(\nabla \cdot \mathbf{u})$$

where the fluid has molecular viscosity, μ [6]. When considering large scale atmospheric flows it is possible to make certain approximations to the momentum equation, resulting in the quasi-geostrophic equations of motion. The approximations rely on the fact that the effects of friction and relative acceleration, $\frac{D\mathbf{u}}{Dt}$, are insignificant compared to the effect of the planet's rotation. To investigate this claim and to begin modifying the momentum equation, we denote the characteristic length, velocity, and time scales as L,U, and τ. Then, notice that

$$\begin{aligned}
\frac{D\mathbf{u}}{Dt} &= \frac{\partial\mathbf{u}}{\partial t} + (\mathbf{u} \cdot \nabla)\mathbf{u} = O\left(\frac{U}{\tau}, \frac{U^2}{L}\right) \\
2\mathbf{\Omega} \times \mathbf{u} &= O\left(2\Omega U\right) \\
\mathbf{F} &= O\left(\frac{\nu U}{L^2}\right)
\end{aligned}$$

This simple scaling argument shows that the ratios of the relative acceleration and friction force to the Coriolis force are

$$\frac{|D\mathbf{u}/Dt|}{2|\mathbf{\Omega} \times \mathbf{u}|} = O\left(\frac{1}{2\Omega\tau}, \frac{U}{2\Omega L}\right)$$

and

$$\frac{|\mathbf{F}|}{2|\mathbf{\Omega} \times \mathbf{u}|} = O\left(\frac{\nu}{2\Omega L^2}\right)$$

implying that both terms become insignificant as the horizontal length scale increases. Equivalently, this is the statement that both the Rossby number and Ekman numbers are small. Now, (1) can be approximated by

$$\rho 2\mathbf{\Omega} \times \mathbf{u} = -\nabla p + \rho g. \tag{2}$$

On letting r, θ, and ϕ be the radius (measured from the center of the planet), latitude, and longitude, equation (2) can be written in component form as

$$\rho(v2\Omega\sin(\theta) - w2\Omega\cos(\phi)) = -\frac{1}{r\cos(\phi)}\frac{\partial p}{\partial \phi} \tag{3}$$

$$\rho 2\Omega u\sin(\phi) = -\frac{1}{r}\frac{\partial p}{\partial \theta} \tag{4}$$

$$-\rho 2\Omega u\cos(\theta) = -\frac{\partial p}{\partial r} - \rho g. \tag{5}$$

Further scaling analysis, taking advantage of the fact that the horizontal length and velocity scales are much larger than that which characterizes the depth of the fluid layer, shows that w is small compared to the horizontal velocities, and that $\rho 2\Omega u\cos(\theta)$ is insignificant compared to the pressure term [6]. Introducing the notation $z = r - r_0$, where r_0 is the radius of the planet, $f = 2\Omega\sin(\theta)$ is the Coriolis parameter, and ρ_s and p_s are the density and pressure fields that would exist in the absence of winds, the approximation to the momentum equation becomes [6]

$$fv = \frac{1}{\rho_s\cos(\theta)}\frac{\partial p}{\partial \phi} \tag{6}$$

$$fu = -\frac{1}{\rho_s r_0}\frac{\partial p}{\partial \theta} \tag{7}$$

$$\rho g = -\frac{\partial p}{\partial z}. \tag{8}$$

Equations (6) and (7) are referred to as the geostrophic approximations to

the momentum equations while (8) is called the hydrostatic equation. The geostrophic equations give a simple relationship between horizontal components of the Coriolis acceleration and the pressure gradient. Unfortunately, there is not enough information contained in this relationship to be useful for atmospheric models. Notice that any given pressure field will determine a reasonable geostrophic, horizontal velocity. So, there is no way to tell whether or not the given pressure field is correct. To obtain more information, it is necessary to reconsider the relative acceleration term, $\frac{D\mathbf{u}}{Dt}$, which is a more significant effect than the viscous term, $\mathbf{F}$, for large scale atmospheric dynamics. By re-introducing the relative acceleration term, the conservation of potential vorticity can be derived and used to model atmospheric dynamics.

Removing the viscosity term from equation (1) and assuming that the horizontal velocities are independent of the height, z, allows for the following definition of the horizontal momentum equation [6]

$$\frac{\partial u}{\partial t} + u\frac{\partial u}{\partial \theta} + v\frac{\partial u}{\partial \phi} - fv = \frac{-1}{\rho}\frac{\partial p}{\partial \theta} \tag{9}$$

$$\frac{\partial v}{\partial t} + u\frac{\partial v}{\partial \theta} + v\frac{\partial v}{\partial \phi} + fu = \frac{-1}{\rho}\frac{\partial p}{\partial \phi}. \tag{10}$$

Also, notice that the continuity equation for a homogeneous, incompressible fluid can be reduced from

$$\frac{\partial \rho}{\partial t} + \mathbf{u} \cdot \nabla \rho = 0$$

to

$$\frac{\partial u}{\partial \theta} + \frac{\partial v}{\partial \phi} = -\frac{\partial w}{\partial z}. \tag{11}$$

by using the fact that ρ is constant throughout the fluid. Let $\zeta = \mathbf{k} \cdot \nabla \times \mathbf{u}$ be the absolute vorticity of the upper, shallow, layer. Subtracting $\frac{\partial}{\partial \phi}$ applied to (9) from $\frac{\partial}{\partial \theta}$ applied to (10) gives

$$\frac{D}{Dt}(\zeta + f) - (\zeta + f)\left(\frac{\partial u}{\partial \theta} + \frac{\partial v}{\partial \phi}\right) = 0. \tag{12}$$

Recall that Jupiter's red spot can be thought of as a nearly two dimensional vortex. Therefore, it is reasonable to think of the red spot as being embedded in a shallow layer of fluid with an upper and a lower boundary. Under this assumption, define H_0 as the average depth of the shallow layer, $h_b(\theta, \phi)$ the rigid bottom of the layer, and $h(\theta, \phi, t)$ as the height of waves that are allowed to deform the layer. Then, $H = H_0 + h - h_b$. Imposing the condition that the horizontal velocities are independent of the height and then integrating (11) over the height of the layer, H, yields

$$\frac{\partial u}{\partial \theta} + \frac{\partial v}{\partial \phi} = \frac{DH}{Dt}\frac{1}{H}.$$

This allows (12) to be written as

$$\frac{1}{\zeta + f}\frac{D}{Dt}(\zeta + f) = \frac{DH}{Dt}\frac{1}{H} \tag{13}$$

or,

$$\frac{D}{Dt}(\ln(\zeta + f)) = \frac{D}{Dt}(\ln(H)),$$

which implies

$$\frac{D}{Dt}\left(\frac{\zeta + f}{H}\right) = \frac{D\Pi}{Dt} = 0. \tag{14}$$

The quantity Π is often referred to as the potential vorticity. Several more simplifications can now be made by allowing for small perturbations of h_b and h around H_0, resulting in the approximation

$$\frac{\zeta + f}{H} \approx \frac{\zeta + f(\theta)}{H_0} - \frac{hf(\theta)}{H_0^2} + \frac{h_b f(\theta)}{H_0^2}$$

Since the horizontal scale of the motion is significantly larger than that of the vertical scale, a locally flat coordinate system centered around the latitude θ_0 is used. The spherical nature of the planet is only taken into account through the variation of the Coriolis parameter with latitude. Linearizing

$f(\theta)$ around a latitude in the center of the horizontal flow, θ_0, yields

$$f \approx f(\theta_0) + \beta_0 y$$

where $\beta_0 = 2\Omega cos(\theta_0)/R_j$, R_j is the radius of Jupiter, and $y = R_j(\theta - \theta_0)$ represents a small change in the latitudinal direction. By substitution into (14), we obtain the quasi-geostrophic β-plane approximation of the potential vorticity [6],

$$\frac{D}{Dt}\left(\frac{\zeta + f(\theta_0) + \beta_0 y}{H_0} - \frac{hf(\theta_0)}{H_0^2} + \frac{h_b f(\theta_0)}{H_0^2}\right) = 0,$$

which implies

$$\frac{D}{Dt}\left(\zeta + \beta_0 y - \frac{hf(\theta_0)}{H_0} + \frac{h_b f(\theta_0)}{H_0}\right) = 0 \tag{15}$$

In geostrophic flow, the horizontal velocity is non-divergent, $\nabla \cdot \mathbf{u}_H = 0$, allowing for the definition of the geostrophic stream function, Ψ. In fact, it can be shown [6] that

$$u = -\frac{g}{f}\frac{\partial h}{\partial \phi}$$

$$v = \frac{g}{f}\frac{\partial h}{\partial \theta}.$$

So, $\Psi = \frac{gh}{f}$ and

$$\zeta = \frac{\partial v}{\partial \theta} - \frac{\partial u}{\partial \phi} = \nabla^2 \Psi.$$

Re-writing (15) in terms of the stream function allows for the following definition of potential vorticity, which is solved more readily when written in polar coordinates, as [5]

$$\zeta_p(r, \phi, t) = \zeta(r, \phi, t) - \beta_0 r - \frac{\Psi(r, \phi, t)}{L_R^2} + \frac{\overline{\Psi}(r)}{L_R^2} \tag{16}$$

where $L_R = \sqrt{gH\Delta\rho/\rho}/f$, ρ is the density, $\Delta\rho$ is the difference in density

between the two layers, g the gravitational acceleration, and the azimuthal velocity of the lower layer is given in terms of the stream function $\overline{\Psi}$. The exact value of $\overline{\Psi}$ is unknown, but based on data obtained from the Voyager missions it is assumed to be time independent [3]. Note that the radial variable, r, has replaced the latitudinal variable, θ. Since Jupiter's red spot is in the planet's southern hemisphere, the choice of sign associated with the term $\beta_0 r$ is consistent with the convention of θ being measured as a positive angle. This implies

$$\frac{D\zeta_p}{Dt} = \left[\frac{\partial}{\partial t} + (\mathbf{u} \cdot \nabla)\right] \zeta_p = 0 \tag{17}$$

where ζ_p is defined as in (16).

2 Numerical Methods

Previous studies have shown that the belt containing the red spot can be thought of as an axis-symmetric, azimuthal flow with almost uniform potential vorticity [3]. Laboratory experiments [7] and numerical simulations show that isolated spots of non-uniform vorticity arise in such flows [3]. Therefore, the numerical simulations discussed in this paper are started with an initial, nearly uniform potential vorticity field containing isolated patches of non-uniformity. The system defined by (16) and (17) is solved on an annulus with inner radius $a = .25$, outer radius $b = 1$, and impermeable boundary conditions, i.e the condition that $\Psi(a, \phi)$ and $\Psi(b, \phi)$ are known and fixed in time.

Given an initial potential vorticity field, equation (16) is solved for the stream function, Ψ, through the use of a Galerkin method. The radial and azimuthal velocties are calculated from the stream function via a one-sided finite difference method. After velocities have been determined, the two dimensional advection equation (17) is solved using an upwinding method. After determining $\zeta_p(r, \phi, t + \triangle t)$, the process is repeated and a new stream function is found through solving (16).

In order to approximate the solution to

$$\nabla^2\Psi - \frac{\Psi}{L_R^2} = q \equiv \zeta_p + \beta r + \frac{\overline{\Psi}}{L_R^2}$$

consider the set of test functions, γ_1, γ_2, ...,γ_n, where

$$\gamma_k = T_n(z)e^{im\phi}$$

with $z = \frac{2r-a-b}{b-a}$ and $T_n(z)$ denoting the nth degree Chebychev polynomial of the first kind. The change of variable $z = \frac{2r-a-b}{b-a}$ is needed to transform the interval $[.25, 1]$ to $[-1, 1]$, where the Chebychev polynomials are defined. The number of test functions depends on the number of grid points used in the radial and azimuthal directions. In simulations discussed in this paper, sixteen points were taken in the radial direction and sixty-four in the azimuthal direction. Instead of solving $\nabla^2\Psi - \frac{\Psi}{L_r^2} = q$, it is required that

$$\left\langle \nabla^2\Psi - \frac{\Psi}{L_R^2} - q, \gamma_k \right\rangle = 0 \qquad \forall k$$

which implies

$$\langle \nabla\Psi, \nabla\gamma_k \rangle - \frac{1}{L_R^2} \langle \Psi, \gamma_k \rangle = \langle q, \gamma_k \rangle \qquad \forall k. \tag{18}$$

The functions Ψ and q are expanded in Fourier modes in the azimuthal direction and Chebychev modes in the radial direction, yielding the following approximations in terms of the test functions, γ,

$$\Psi \approx \sum_n \sum_m C_{n,m} T_n(z) e^{im\phi} = \sum_j c_j \gamma_j \tag{19}$$

$$q \approx \sum_n \sum_m B_{n,m} T_n(z) e^{im\phi} = \sum_j b_j \gamma_j \tag{20}$$

where the $B_{n,m}$ can be found from the known forcing term, $C_{n,m}$ are unknown, and the coefficients b_j are simply a reordering of the $B_{n,m}$. Transitions between transform space and real space can be accomplished through the use of

the fast Fourier transform and the following Chebychev transformation matrices. The first $N+1$ coefficients in the Chebyshev expansion of a function on [a,b] are determined from the value of the function at the $N+1$ Gauss-Lobatto points defined by $x_n = \frac{a+b}{2} + \frac{b-a}{2}\cos(n\pi/N)$ for $n = 0, 1, ..., N$. Given a column vector of function values at the appropriate Gauss-Lobatto points, define the Chebychev transformation matrices [1]

$$CT_{ij} = \cos\left(\frac{\pi jk}{N}\right)$$

$$ICT_{ij} = \frac{2}{N\overline{c}_k\overline{c}_j}\cos\left(\frac{\pi jk}{N}\right)$$

where $\overline{c}_j = 2$ if $j = 0, N$ and $\overline{c}_j = 1$ otherwise. Then, CT applied to $\vec{F}$ will give a column vector of the first $N+1$ Chebychev coefficients. The matrix ICT is the inverse of CT and will transform a column of Chebychev coefficients into the real space function values at the corresponding Chebychev nodes. Substituting (19) and (20) into equation (18) allows for the stream function problem to be written in matrix form as

$$\left(K - \frac{1}{L_r^2}R\right)\vec{U} = R\vec{Q} \tag{21}$$

where $U_i = c_i$, $Q_i = b_i$, $K(k,j) = \langle \nabla\gamma_k, \nabla\gamma_j \rangle$, and $R(k,j) =< \gamma_k, \gamma_j >$. Due to the orthogonality of the functions $e^{ik\phi}$ and $e^{ij\phi}$ on the interval $[0, 2\pi]$, the matrices K and R are sparse. In fact, making the identification

$$c_j = T_{j \bmod 16} e^{i\lceil \frac{j}{16} \rceil \phi},$$

the matrices R and K both take on simple block structures. More specifically,

$$\mathbf{K} = \begin{pmatrix} K^{(1)} & 0 & 0 & 0\ldots \\ 0 & K^{(2)} & 0 & 0\ldots \\ 0 & 0 & K^{(3)} & 0\ldots \\ \vdots & \vdots & \vdots & \ddots \end{pmatrix} \qquad \mathbf{R} = \begin{pmatrix} R^{(1)} & 0 & 0 & 0\ldots \\ 0 & R^{(2)} & 0 & 0\ldots \\ 0 & 0 & R^{(3)} & 0\ldots \\ \vdots & \vdots & \vdots & \ddots \end{pmatrix}$$

where $K^{(j)}$ is a 16×16 block and $K^{(j)} = K^{(k)}$. With the current identification between c_j and γ_j each block is associated with a fixed wave number from the relevant trial functions. The matrix R has the same structure, but $R^{(j)}$ differs from $R^{(k)}$ by a constant factor dependent upon the wave numbers in the associated trial functions. The single matrix equation (21) can be broken up by solving the sixty-four separate matrix equations suggested by the above block decomposition.

With the system written in this form, it is easier to impose the boundary conditions $\Psi(a,\phi) = \eta_1$ and $\Psi(b,\phi) = \eta_2$. Let b_0 and b_1 denote the first and last rows of the matrix CT respectively. Then, in terms of the coefficients, $\vec{U}$, the boundary conditions imply $b_0\vec{U}^{(j^*)} = \eta_1$ and $b_1\vec{U}^{(j^*)} = \eta_2$ where j^* denotes the block matrix associated with the 0th Fourier mode. The constraints imposed on the other blocks are trivial since the values of Ψ on the boundary should have no oscillating components. All nontrivial information is stored in the 0th Fourier mode. Define $V^{(j)} = K^{(j)} - \frac{1}{L_R^2}R^{(j)}$ and $G^{(j)} = R^{(j)}Q^{(j)}$. The constraints set by the boundary conditions can be imposed by introducing the Lagrange multipliers, λ_1 and λ_2, and solving the system

$$\begin{pmatrix} V^{(j)} & b_0^T & b_1^T \\ b_0 & 0 & 0 \\ b_1 & 0 & 0 \end{pmatrix} \begin{pmatrix} U^{(j)} \\ \lambda_1 \\ \lambda_2 \end{pmatrix} = \begin{pmatrix} G^{(j)} \\ \overline{\eta}_1 \\ \overline{\eta}_2 \end{pmatrix} \tag{22}$$

with

$$\overline{\eta}_1 = \begin{cases} \eta_1 & \text{if } j = j^* \\ 0 & \text{if } j \neq j^* \end{cases} \qquad \overline{\eta}_2 = \begin{cases} \eta_2 & \text{if } j = j^* \\ 0 & \text{if } j \neq j^* \end{cases}$$

to get the needed fourier-chebychev expansion coefficients, which are used to reconstruct an approximation of the stream function, Ψ. Recall that $\mathbf{u} = \left(\frac{1}{r}\frac{\partial\Psi}{\partial\phi}, \frac{-\partial\Psi}{\partial r}\right) = (v_r, v_\phi)$. So, v_r and v_ϕ are determined from Ψ through a

one-sided finite difference method, allowing for equation (17) to be re-written in polar coordinates as

$$\frac{\partial \zeta_p}{\partial t} + v_r \frac{\partial \zeta_p}{\partial r} + \frac{v_\phi}{r} \frac{\partial \zeta_p}{\partial \phi} = 0$$

In upwinding, a one sided finite difference method is used to approximate the spatial derivatives of ζ_p. For stability purposes, a forward difference is taken to approximate $\frac{\partial \zeta_p}{\partial r}$ at a given point, (r_i, ϕ_j), if $v_r(r_i, \phi_j) < 0$. Conversely, a backward difference is used if $v_r(r_i, \phi_j) > 0$. Derivatives in the azimuthal direction are estimated similarly and the time derivative is approximated by the forward euler method.

3 Results

Define $\tilde{v}_\phi$ as the original azimuthal flow that is superposed with spots of vorticity. Let ζ_e denote the difference between the ζ_p produced from original azimuthal flow, $\tilde{v}_\phi$, and the ζ_p of a spot of vorticity. Define the shear of the flow by $\sigma(r,t) = r\partial(\tilde{v}_\phi/r)/\partial r$. Consider the case where $L_r \to \infty$. Then in order to initially satisfy (16), $\tilde{v}_\phi$ must be of the form $\beta r^2/3 + C/r$. Equations (16) and (17) are solved in the case where $L_r \to \infty$, $\tilde{v}_\phi(r, t = 0) = \beta r^2/3 + C/r$, $\beta = 1$, $C = 1/6$. The function $\Psi(r, \phi, t = 0)$ is determined explicitly from the relation $\frac{-\partial \Psi}{\partial r} = v_\phi$ and used to set the boundary conditions (which remain fixed for all time). Results of trials using this setup are summarized in figures 1-3.

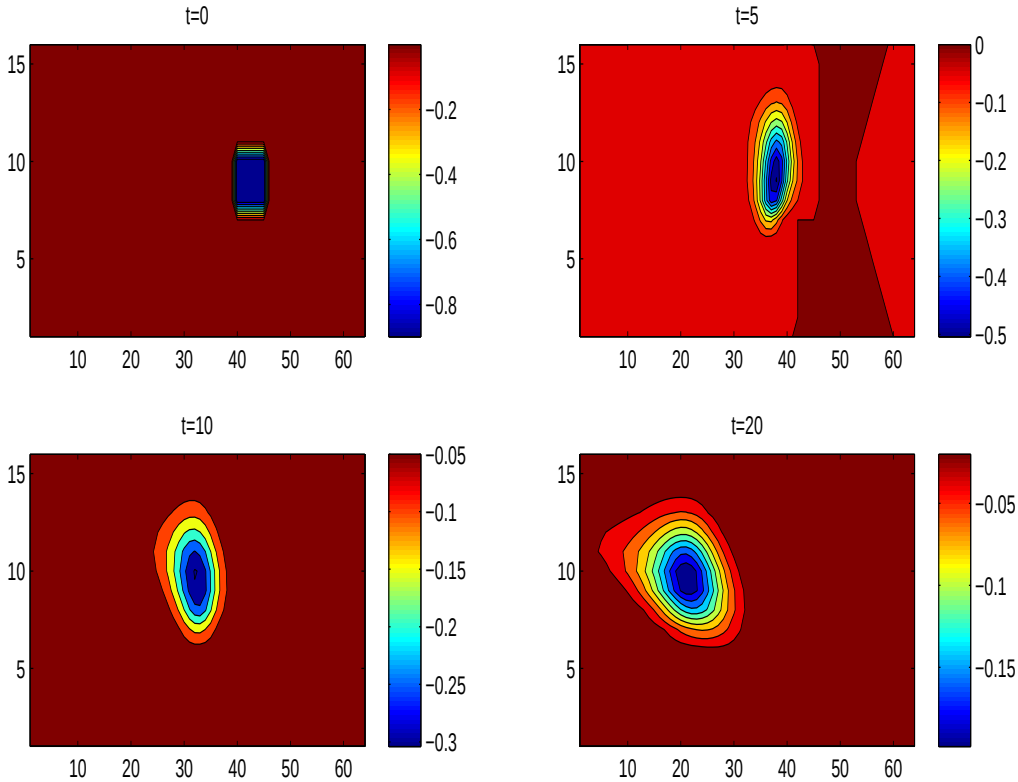

Figure 1: A spot with $\zeta_e = -.9$ at times $t = 0$, $t = 5$, $t = 10$, and $t = 20$ from upper left to lower right.

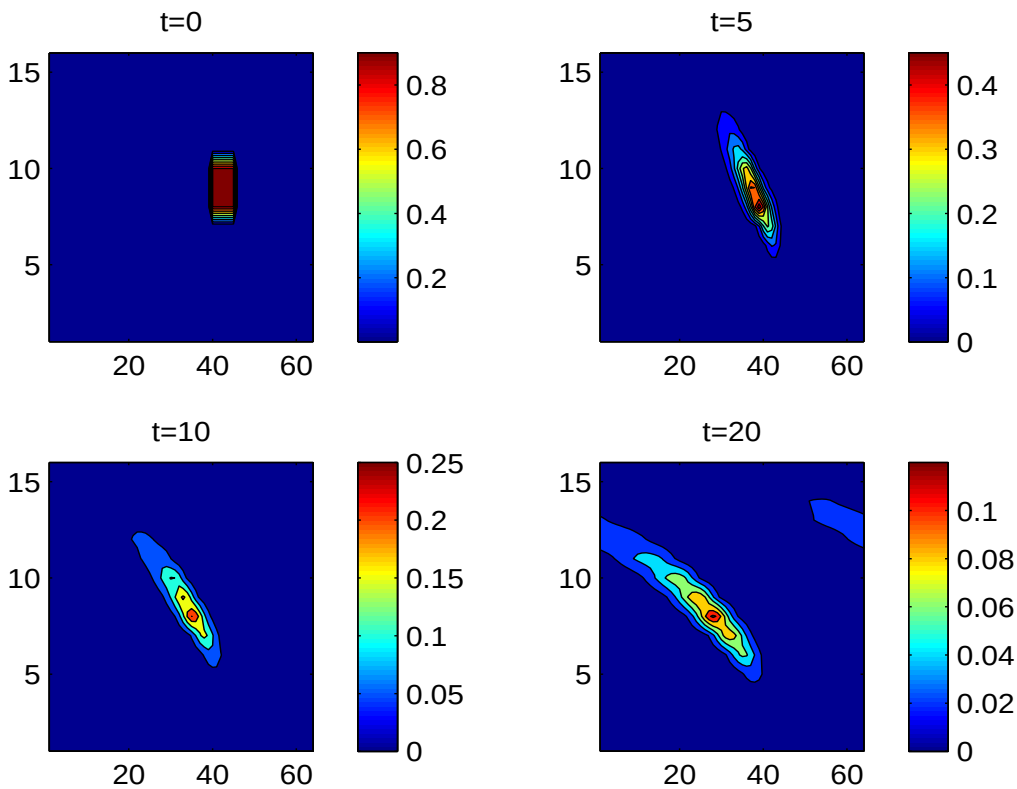

Figure 2: A spot with $\zeta_e = .9$ at times $t = 0$, $t = 5$, $t = 10$, and $t = 20$ from upper left to lower right.

In figure (1) the spot superposed in the flow has $\zeta_e = -.9$ while in figure (2) the spot has $\zeta_e = .9$. Note that the shear is given by $\sigma(r, t = 0) = 1/3(r - 1/r^2)$, which is negative throughout the entire domain. Figures (1) and (2) suggest that a spot with the same sign as the shear is able to maintain its structure, or is stable, while a spot having the opposite sign is unstable. The unstable spot becomes elongated with both ends being pushed towards the boundaries. Notice the decrease in the amount of ζ_e present in the spot as time increases. The stable spot appears to hold its shape, but there is still a loss in the total amount of ζ_e in the system. Figure (3) shows the merger of two stable spots, both of which have $\zeta_e = -.9$.

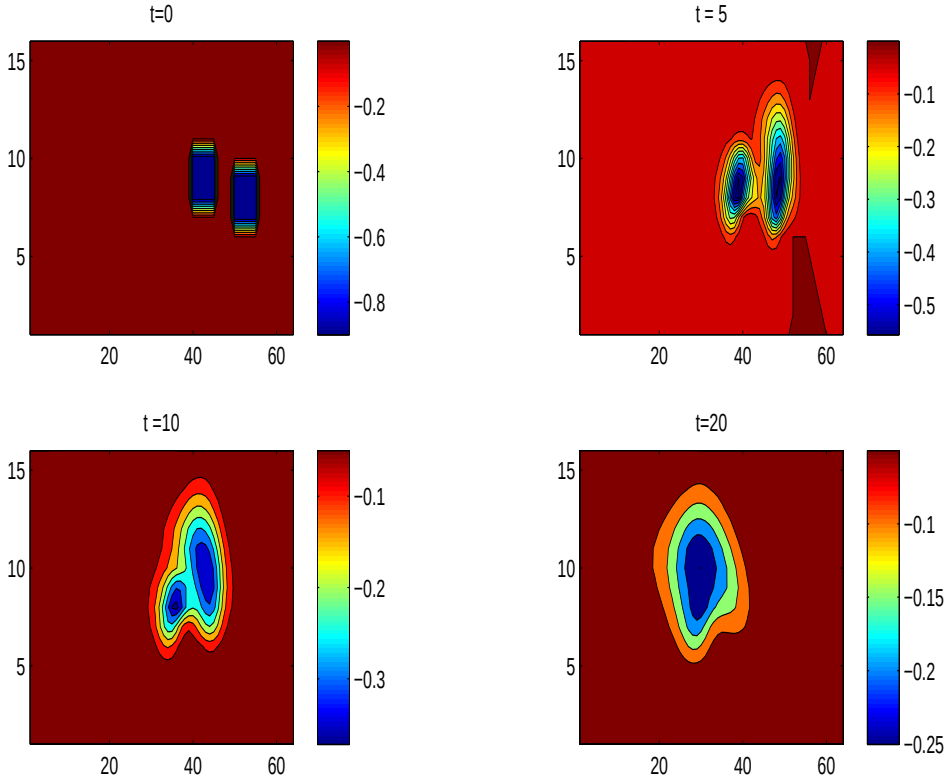

Figure 3: A spot with $\zeta_e = -.9$ at times $t = 0$, $t = 5$, $t = 10$, and $t = 20$ from upper left to lower right.

At first spots are drawn towards each other due to differential rotation [5]. The rotation of the down-stream spot pushes the second spot closer to the radial boundary. Since the flow is faster for larger values of r, the second spot will catch up and the two will merge into a larger, stable spot.

4 Conclusion

Data suggests the expected results, which are similar to those obtained by Marcus [3]. Marcus found that spots having the same sign as the shear were stable and those having a different sign were unstable. This is not surprising

as shear would be expected to inhibit rotation if directed opposite to the sense of rotation. Previous studies also demonstrate the merger of separate stable spots as well as an unstable spot evolving into an elongated string-like shape with the inner and outer ends being pushed towards the inner and outer boundaries respectively [3]. The results shown here tend to support those findings, even though the numerical methods used in this study are not as accurate as those used by Marcus [4].

One concern with the current method is the apparent dissipation of potential vorticity with time. It is not surprising that a loss of ζ_e occurs in the unstable case where the spot quickly elongates and decays. The loss in ζ_e could be attributed to the ζ_e moving to scales too small to be resolved by the spatial resolution of the model. In the stable case, ζ_e also decays, but not as quickly. A certain amount of dissipation is expected, but more time is needed to determine whether or not the demonstrated loss of ζ_e is realistic.

Results suggest that it is possible to create a simple model for large Jovian vortices, such as the red spot, using quasi-geostrophic theory. Improvements to the model would include a more accurate advection scheme and inclusion of the three dimensional properties of the red spot. Simulations show that the merger of several spots can create a larger, stable spot, which could help to explain the persistence and size of a vortex such as Jupiter's Great Red Spot.

5 Acknowledgments

I would like to thank Dr. Shankar Venkataramani for his time and help with this project.

References

[1] Canuto, C., Hussaini, M.Y., Quarteroni, A., Zang, T.A., *Spectral Methods: Fundamentals in a Single Domain* (2006).

[2] Holton, J, *Introduction to Dynamic Meteorology* (Academic Press, 2004).

[3] Marcus, P.S., Numeical Simulation of Jupiter's Red Spot, *Nature*. **331** 693-696, (1988).

[4] Marcus, P.S. *Numerical Analysis* (eds Griffiths, D. F. and Watson, G. A.) 125-139, (1986).

[5] Marcus, P.S., Jupier's Red Spot and Other Vortices, *Annu. Rev. Astron. Astrophys*. **31** 223-273, (1993).

[6] Pedloski, J, *Geophysical Fluid Dyanmics* (1986).

[7] Sommeria, J, Meyers, S.D, Swinney, H.L., Laboratory Simulation of Jupiter's Great Red Spot, *Nature*. **331** 689-693, (1988).

[8] Zdunkowski, W., Andreas B. *Dynamics of the Atmosphere* (Cambridge University Press, 2003)